



國立中山大學材料與光電科學學系

博士論文

Department of Materials and Optoelectronic Science

National Sun Yat-sen University

Doctoral Dissertation

氧化鉻摻雜鋯之鐵電記憶體物理機制研究

Investigation on the Physics Mechanism of Zr:HfO₂ Ferroelectric

Memory

研究生：陳穩仲

Wen-Chung Chen

指導教授：蔡宗鳴 博士

Dr. Tsung-Ming Tsai

中華民國 112 年 1 月

January 2023



國立中山大學材料與光電科學學系

博士論文

Department of Materials and Optoelectronic Science

National Sun Yat-sen University

Doctoral Dissertation

氧化鉻摻雜鋯之鐵電記憶體物理機制研究

Investigation on the Physics Mechanism of Zr:HfO₂ Ferroelectric

Memory

研究生：陳穩仲

Wen-Chung Chen

指導教授：蔡宗鳴 博士

Dr. Tsung-Ming Tsai

中華民國 112 年 1 月

January 2023

論文審定書

國立中山大學研究生學位論文審定書

本校材料與光電科學學系博士班

研究生陳穩仲（學號：D053100011）所提論文

氧化鎵摻雜鋯之鐵電記憶體物理機制研究

Investigation on the Physics Mechanism of Zr:HfO₂ Ferroelectric Memory

於中華民國 111 年 12 月 11 日經本委員會審查並舉行口試，符合博士學位論文標準。

學位考試委員簽章：

召集人 莫亦先 莫亦先 委員 蔡宗鳴 蔡宗鳴

委員 張鼎張 張鼎張 委員 陳紀文 陳紀文

委員 陳柏勳 陳柏勳 委員 _____

委員 _____ 委員 _____

委員 _____ 委員 _____

指導教授（蔡宗鳴） 蔡宗鳴 (簽名)

誌謝

在中山大學 10 年的時間，轉眼已進入到尾聲，很幸運能在大二下學期遇見了張鼎張老師，開啟了忙碌且充實的博士班生活。首先非常感謝我的指導教授張鼎張老師，老師總能將艱澀難懂的半導體元件物理知識，化為簡單常見的生活比喻，帶我們快速跨過知識門檻，迅速融入實驗室。在實驗方面，老師提供全國最完善的量測設備並與各大公司進行產學合作，讓我們所學實際用來解決業界問題，更能將這過程發表至國際期刊，在此對張鼎張老師致上最誠摯的敬意與感謝。此外，我也很感謝材光系的指導教授，蔡宗鳴老師，謝謝老師在研究及論文上的指導，使我能順利完成博士論文。感謝口試委員海軍官校陳柏勳老師、台積電莫亦先經理及奈盾科技陳紀文董事長撥冗審查，並在口試時適時給予指正與教導，特此感謝。

在博士班生活中，感謝所有實驗室大家的陪伴。其中特別感謝信儒學長與志承學長用心地指導我；非常謝謝柏勳學長在研究及國際期刊撰寫上給予指導與討論；謝謝志承學長與志陽在專利上的指導與訓練；謝謝敏甄學姐在公共事務上給予相當大的幫助。非常感謝在博士班期間所幫助我的天健、致宏、柏詠、郁庭、穎新、孝承、懿霆、俞慶、宏誌、馨平、政憲、智程等學長姊在研究上的指導及鼓勵，與碩士班學長姐：德翔、貞頤、証期、文彥、伶宜、富宸、俐卉等，以及同學們：皓軒、宇哲、俊曲、福源、揚豪、好珊、豐閔、郁碩，以及學弟妹：仕鎧、建傑、珮瑜、煒宸、詠方、笠荃、詠慈、娟瑋、又瑄、重緯、聖堯、泓邑、沛君、裕博，謝謝各位在實驗及公共事務上的協助，也感謝大家的陪伴，讓我博士班生活帶來許多歡笑的回憶。

另外也要感謝材光系老師郭紹偉教授、蘇威宏教授、張六文教授、沈博彥教授、高伯威教授、郭哲男助理教授等，材光系辦顏秀芳小姐、陳秀玉小姐、林慧婷小姐、王淑敏小姐、張羽萱小姐等，協助我解決各種系上大小事。另外也要感謝 FIB 負責人彥文學長、TEM 負責人惠君學姊、奈米核心書香姐

及奈米中心惠華姐，讓我靈活運用各種分析與製程儀器。

最後我要感謝我的家人，父親陳文德先生、母親姜夙芬女士、姐姐陳品瑄及妹妹陳芷芸，謝謝你們在我念書期間一路上的支持與陪伴，讓我能順利完成博士學位，進入人生下一階段。在此也感謝國防工業發展基金會提供獎學金，讓我在博士班就讀期間沒有經濟負擔。接下來要進入下個階段，我將帶著感恩的心繼續努力前進，再次感謝每一位幫助過我的人。

陳穩仲 謹識

摘要

隨著大數據、人工智慧及物聯網等科技蓬勃發展，電子產品的運算速度及數據存取能力日益受到重視，因此高效能運算晶片及記憶體儲存元件的開發是勢在必行。氧化鉻基底 (HfO_2 -based) 鐵電記憶體(Ferroelectric Random Access Memory, FeRAM)與傳統鐵電材料 $\text{SrBi}_2\text{Ta}_2\text{O}_9$ (SBT)或 $\text{Pb}(\text{ZrTi})\text{O}_3$ (PZT)相比，寫入速度快、穩定性高、可微縮性高且與半導體製程匹配。然而， HfO_2 基底的鐵電記憶體目前仍存在幾項瓶頸，包含操作電壓過高、記憶窗口不足及操作前需多次喚醒(wake up)。

本研究為了解氧化鉻基底鐵電記憶體的傳導機制並了解缺陷對鐵電記憶體的影響，針對不同製程溫度的鐵電薄膜與不同電極製備的鐵電記憶體做比較，透過材料分析與電性量測，建立鐵電記憶體的物理模型，進一步設計出高性能與高可靠度的鐵電記憶體。

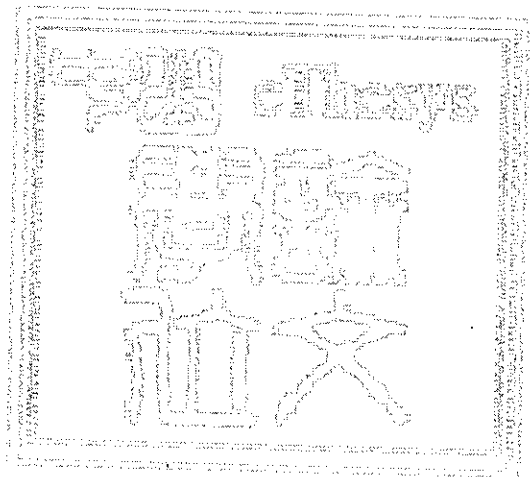
在第三章中，針對鐵電記憶體元件結構成分進行材料分析，搭配電性量測分析鐵電記憶體的 I-V、C-V、與 P-V，並透過變溫實驗確認了鐵電記憶體的轉態機制。因為在低電流的情況是不隨溫度變化的 Fowler-Nordheim 穿隧機制，在高電流狀態下為隨著溫度升高電流會變大的蕭特基機制，根據這些實驗結果，提出一個能帶模型解釋這個現象。

在第四章中，針對高溫與低溫原子層沉積製程的鐵電記憶體分析，根據電性與材料分析結果，低溫製程的鐵電記憶體擁有較好的性能，有較大的晶粒，在相同面積下，擁有大晶粒的缺陷較少，極化值高，根據實驗結果，我們提出一個模型解釋這現象。

在第五章中，針對半導體製程材料常用的 TiN 與 TaN 電極作為鐵電記憶體的電極分析兩者在性能與可靠度的差異，TaN 比較匹配 HZO 薄膜的晶格常數，因此 TaN 電極的鐵電記憶體在喚醒前有較高的極化值與低漏電流。然而，漏電流在經過喚醒過程後顯著上升，經過電流機制擬和分析出 Poole-Frenkel 傳導機制，根據

這些實驗結果與 TiN 電極的元件做比較提出一個氧空缺的模型解釋。

關鍵字：鐵電記憶體、高性能記憶元件、沉積溫度、電流傳導機制、切換物理模型、晶粒大小



Abstract

With the rapid advancement of technologies like big data, artificial intelligence, and the Internet of Things, the attention of the world has shifted more and more toward the computational power and the data access capabilities of electronic goods. Therefore, the development of high-performance computing chips and memory storage devices is imperative. Compared to traditional ferroelectric materials, such as $\text{SrBi}_2\text{Ta}_2\text{O}_9$ (SBT) or PbZrTiO_3 (PZT), the HfO_2 -based ferroelectric random access memory (FeRAM) owns a smaller switching voltage, high writing speed, high stability and high shrink ability and is compatible to the usual semiconductor fabrication process as well. However, the HfO_2 -based FeRAM still exhibits some bottlenecks, including higher operation voltage, insufficient memory windows and the wake-up process needed before operation.

In this study, in order to understand the conduction mechanism of hafnium oxide-based ferroelectric memory and the influence of defects on ferroelectric memory, the characteristics of ferroelectric memory with ferroelectric films at different temperatures or with different electrodes are compared. A physical model of ferroelectric memory is established through the material analysis and the electrical measurements, and ferroelectric memory with high performance and high reliability is further designed.

In Chapter 4, the material analysis is performed for the structure confirmation of ferroelectric memory, and the electrical measurements including current-voltage (I-V), capacitance-voltage (C-V) and polarization-voltage are taken to analyze the ferroelectric memory. Also, the experiments are conducted at various temperatures to help verify the transport mechanism. The low current transport by the F-N tunneling mechanism does not change with temperature, whereas the high current transport via the Schottky mechanism increases with temperature increasing. According to these experiments, a band model is proposed to explain the electron transport in the HZO ferroelectric memory.

In Chapter 5, the ferroelectric memory is fabricated at high and low temperatures in the atomic layer deposition (ALD) process. It is known from the electrical and material analyses that the LTD-FeRAM exhibits better performance and larger grains. Within the same area of the device, therefore, the larger grain would have fewer grain boundaries to cause a smaller number of charge defects. According to the experiments, a model is proposed to explain this phenomenon.

In Chapter 6, this study investigates the difference in electrical performance and reliability with either TiN or TaN applied. Both are commonly used in semiconductor process materials, as the electrode material in ferroelectric random access memories with the same ferroelectric layer of $\text{Hf}_{0.5}\text{Zr}_{0.5}\text{O}_2$ (HZO). Because the lattice constant of TaN is better matched to HZO, the TaN-electrode device possesses larger remnant polarization, higher capacitance and lower leakage before the wake up. However, the leakage current of the TaN-electrode device increases significantly after the wake up. To figure out this phenomenon, current fitting is implemented. The results indicate that electrons of the TaN-electrode device conduct through the oxygen vacancies by Poole-Frenkel emission. Based on these experimental results, an oxygen vacancy model is proposed to compare with the TiN electrode devices.

Keywords: Ferroelectric Memory, High Performance Memory Device, Deposition Temperature, Current Conduction Mechanism, Switching Physics Model, Grain Size

Contents

論文審定書	i
誌謝	ii
摘要	iv
Abstract	vi
Figure Captions	x
Table Captions	xiii
Chapter 1. Introduction	1
1-1. Overview of memory.....	1
1-2. Research Motivation.....	2
Chapter 2. Literature Review.....	3
2-1. Advanced Memory.....	3
2-2. Carrier Conduction Mechanism for MIM device.....	11
Chapter 3. Instrument Introduction.....	19
Chapter 4. Current Conduction Mechanism of HfZrO_x Ferroelectric Memory	23
4-1. Motivation.....	23
4-2. Experimental Setup	23
4-3. Results and Discussion.....	26
4-4. Summary.....	36
Chapter 5. Different Deposition Temperature of Ferroelectric Layer.....	37
5-1. Motivation.....	37
5-2. Experimental Setup	38

5-3. Results and Discussion.....	41
5-4. Summary.....	48
Chapter 6. Different electrode effect in Degradation Behavior	49
6-1. Motivation.....	49
6-2. Experimental Setup	51
6-3. Results and Discussion.....	52
6-4. Summary.....	60
Chapter 7. Conclusion.....	61
Reference	63
Appendix	74
Publication List.....	74

Figure Captions

Chapter 2

Fig. 2 - 1 The operation of PCRAM	4
Fig. 2 - 2 The stucture of PCRAM	4
Fig. 2 - 3 MRAM operation principle and structure	5
Fig. 2 - 4 RRAM structure and forming process	6
Fig. 2 - 5 RRAM operation model	7
Fig. 2 - 6 The operation of FeRAM.....	9
Fig. 2 - 8 Schematic diagram of the energy band of the Schocky emission mechanism	13
Fig. 2 - 9 Schematic diagram of the energy band of the Poole-Frenkel emission mechanism	14
Fig. 2 - 10 Schematic diagram of the energy band of the direct tunneling mechanism.	16
Fig. 2 - 11 Schematic diagram of the Hopping conduction band of electrons.	18

Chapter 3

Fig. 3 - 1 Multifunctional semiconductor measurement and analysis system.....	20
Fig. 3 - 2 Multifunctional semiconductor measurement and analysis system.....	20
Fig. 3 - 3 Low-temperature semiconductor measurement platform.	21
Fig. 3 - 4 The temperature range can reach 4K~400K. It can also measure various atmospheres (such as nitrogen, water, alcohol, NO and CO).....	22

Chapter 4

Fig. 4- 1 (a) The structure of the HfZrO _x -based MFM capacitor. (b)TEM cross-section,	
--	--

(c) mapping and (d) elemental proportion of HfZrO _x -based MFM capacitor	25
Fig. 4- 2 HRTEM images and the corresponding diffraction patterns for the HfZrO _x -based MFM capacitor.	26
Fig. 4- 3 The I-V characteristics of HfZrO _x -based MFM capacitor at different temperatures. The arrow indicates increasing current as the temperature increases, while X represents unchanging current as the temperature increases.	27
Fig. 4- 4 The dielectric constant of HfZrO _x -based MFM capacitor at different temperatures.....	28
Fig. 4- 5 The polarization of HfZrO _x -based MFM capacitor at different temperatures.29	

Chapter 5

Fig. 5- 1 The process flow and device structure of the HfZrO _x ferroelectric memory.39	
Fig. 5- 2 The TEM EDS line scan of LTD-FeRAM and HTD-FeRAM.	40
Fig. 5- 3 The C-V measurement of (a) LTD-FeRAM and (b) HTD-FeRAM.....	42
Fig. 5- 4 The P-V measurement of (a) LTD-FeRAM and (b) HTD-FeRAM.	43
Fig. 5 - 5 Comparison of LTD-FeRAM and HTD-FeRAM for (a) I-V and (b) P-V measurements.Different frequency C-V measurements for (c) LTD-FeRAM and (d) HTD-FeRAM.	44
Fig. 5 - 6 The endurances of (a) LTD-FeRAM and (b) HTD-FeRAM.	45

Chapter 6

Fig. 6 - 1 Cross-sectional TEM image of (a) TiN/HZO/TiN and (b) TaN/HZO/TaN devices. (c) Polarization hysteresis loops at cycle 104. Endurance reliability tests corresponding to HZO-based MFM capacitors with (d) TiN and (e) TaN electrodes. 52	
---	--

Fig. 6 - 2 (a) C-V characteristics and (b) retention reliability tests of FeRAM for TiN and TaN electrodes. I-V curves of two devices measured (c) before and (d) after wake up effect.....	54
Fig. 6 - 3 Fitting results of (a) Schottky emission and (b) Poole-Frenkel current conduction mechanism for TiN- and TaN-electrode FeRAMs, respectively.....	55
Fig. 6 - 4 (a) The influence of temperature on the fitting results of I-V characteristics, which confirms Poole-Frenkel emission mechanism for TaN-electrode device. (b) Linear relationship between $\ln(I/V)$ and $1000/T$ for 1.4 V to 1.8 V. Accordingly, the extracted trap level is 0.65 eV.....	57
Fig. 6 - 5 Model schematics of behavior during operating process until breakdown for (a)(b)(c) TiN-electrode FeRAM and (d)(e)(f) TaN-electrode FeRAM.....	59

Table Captions

Chapter 2

Table 2-1. Comparison of Ferroelectric embedded Memory with traditional Memory 8